

# The thin sectional anatomy of the temporal bone correlated with multislice spiral CT

Junping Zhen · Cheng Liu · Shaoyu Wang ·  
Shuwei Liu · Jingzhen He · Jun Wang · Haisong Chen

Received: 22 October 2006 / Accepted: 23 May 2007 / Published online: 22 June 2007  
© Springer-Verlag 2007

**Abstract** The aim of this study was to explore the method for obtaining the thin sectional anatomy data of the adult temporal bone and study the fine structures using this method. Three fresh adult cadaveric heads were scanned with multi-slice computer tomography (MSCT) centered on petrous bones. The CT images of 0.6 mm were obtained by multi-planar reformation (MPR). The slices of 0.1 mm were shaved off the specimen in the axial direction with the numerical control milling machine after being embedded and frozen, pictures of which were taken by the digital camera and saved in the computer. The thin axial sectional anatomic structures of the intra-temporal were investigated and correlated with MPR images. Via the comparison, fifty micro-anatomic structures of the temporal bone that can't be delineated clearly or missed in the thick sections were evaluated. The anatomical details of the temporal bone can be clearly delineated in MSCT in sub-millimeter and were identical to those in sectional anatomy images. This method can supply anatomical details that had been missed or overlooked for imaging diagnosis and surgical anatomy.

**Keywords** Temporal bone · Sectional anatomy · Numerical control milling technique · Multi-slice CT

## Introduction

The temporal bone is a small, but complicated structure, which contains the organs of hearing and balance. The facial nerve, internal carotid artery and internal jugular vein are also located in it. Knowledge of the topography of these structures and their mutual relationships is essential in any surgical approach to the temporal bone. Diagnosis of diseases in these important regions requires adequate clinical information as well as a thorough knowledge of normal temporal bone anatomy [1, 3, 5, 6, 8, 9, 13, 16, 18, 24]. In previous studies, the normal sectional anatomy was illustrated by macro-sections of the temporal bone obtained in the axial plane. Each section was then compared with the corresponding CT image. However, all macro-sections from the cadavers, and the CT images are from other studies on living species. This explains why the CT sections are similar but not identical to the corresponding macro-sections. Recent advances in multi-slice CT including the development of scanners with 32 detector rows, allow the acquisition of isotropic voxels that can be reconstructed in any plane of section [1, 3, 8, 11]. It gives radiologists the opportunity to visualize the micro-anatomic structures of the middle and inner ear in greater detail and may help to increase the accuracy of CT for the diagnosis of diseases of the middle and inner ear. But if we want to discriminate and analyze the CT images of the temporal bone, we still need to depend on sectional anatomy [10, 13]. In this article we dissected the temporal bone into thin segments of sub-millimeter, and described the relevant radiological anatomy.

---

J. Zhen · S. Liu · J. He  
Shandong University, Jinan, Shandong, China

C. Liu · S. Wang · H. Chen  
Shandong Medical Imaging Research Institute,  
Jinan, Shandong, China

J. Wang  
Shanxi Medical University, Shanxi, China

C. Liu (✉)  
CT Department, Shandong Medical Imaging Research Institute,  
324 jingwu road, Jinan, Shandong 250021, China  
e-mail: zhenjunping04@sohu.com

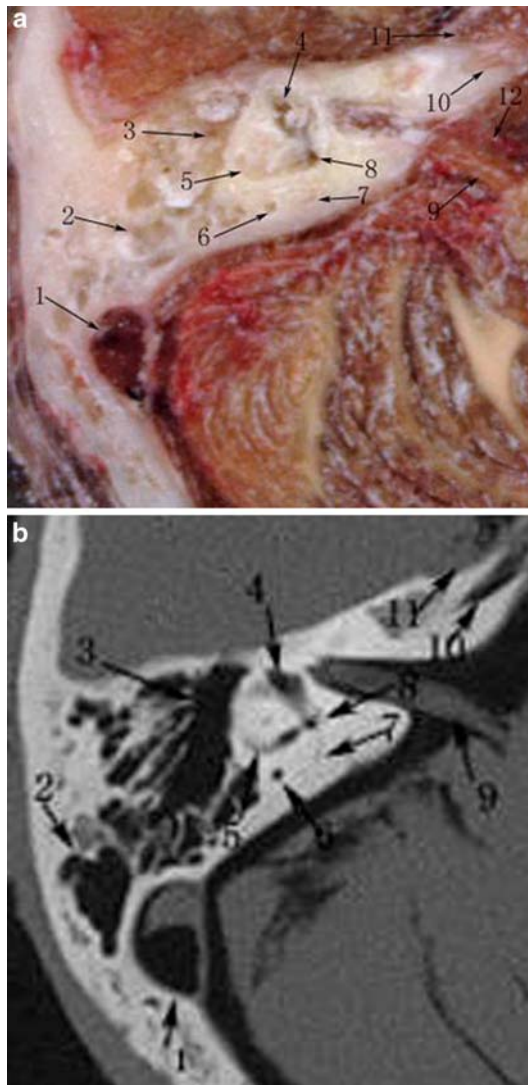


**Fig. 1** **a** Section of the vestibular aqueduct. **b** CT corresponding to **a**. 1 sigmoid sinus, 2 mastoid cells, 3 atticus, 4 vestibule, 5 lateral semicircular canal, 6 arcus of lateral semicircular canal, 7 vestibular aqueduct, 8 common bony crus, 9 nervus statoacusticus, 10 carotid canal, 11 Meckel' cave, 12 labyrinthine artery

The methods can supply anatomical details that had been missed or overlooked in previous studies.

### Materials and methods

Three fresh adult cadaveric heads without organic lesions verified by naked-eye observation were scanned by MSCT (Somatom sensation cardiac 64, Siemens, Germany). Each subject was kept supine on the CT bed, and the horizontal reference was the superior orbitomeatal line. The scanning ranged from the emergence of the petrous pyramid to the mastoid. The scanner was equipped with 32 rows of detec-

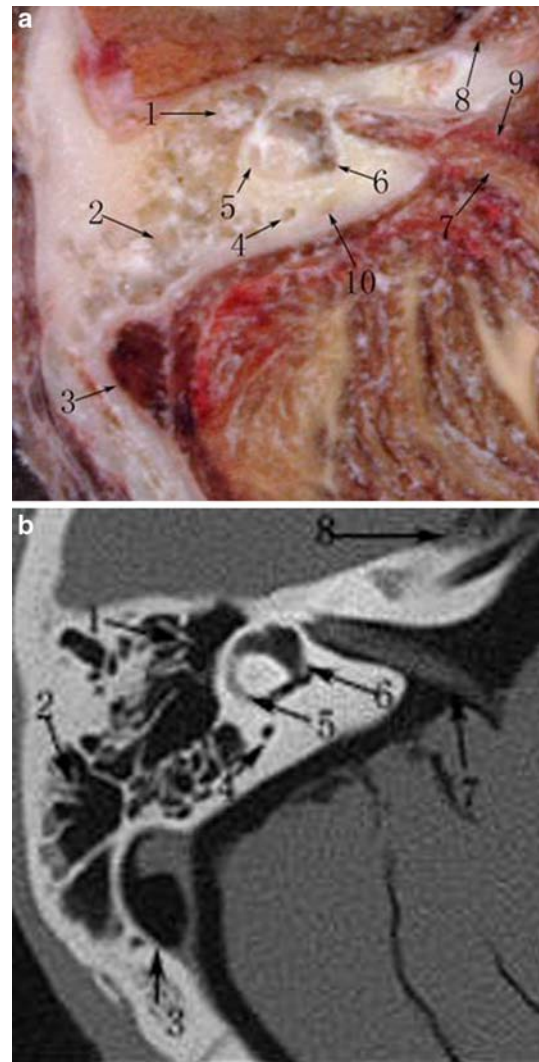


**Fig. 2** **a** Section of the lateral semicircular canal. **b** CT corresponding to **a**. 1 atticus, 2 mastoid air cell, 3 sigmoid sinus, 4 posterior semicircular canal, 5 lateral semicircular canal, 6 vestibule, 7 nervus statoacusticus, 8 Meckel' cave, 9 labyrinthine artery, 10 vestibular aqueduct

tors, but the use of an oscillating focal spot produces the effect of scanning with 64 detector rows. The scanning was performed in the standard axial plane with helical technique (120 kV, 350 mA, pitch of 0.85, rotation time of 1 s, section thickness of 0.6 mm, matrix  $512 \times 512$ , FOV300 mm). The image data set was reconstructed to an 80-mm field of view, with an individual voxel size of  $0.6 \times 0.6 \times 0.6$  mm, and then we used a workstation (wizard Siemens) to get the MPR images.

The specimen was located and marked by the infrared ray of the CT when the CT scan was performed. After marking and measurement, it was fixed in frame and then placed in a low temperature room for a 5-day cry preservation, 2 days in  $-20^\circ$ , 2 days in  $-30^\circ$ , 1 day in  $-40^\circ$ . The specimen was put into a self-made container and embedded

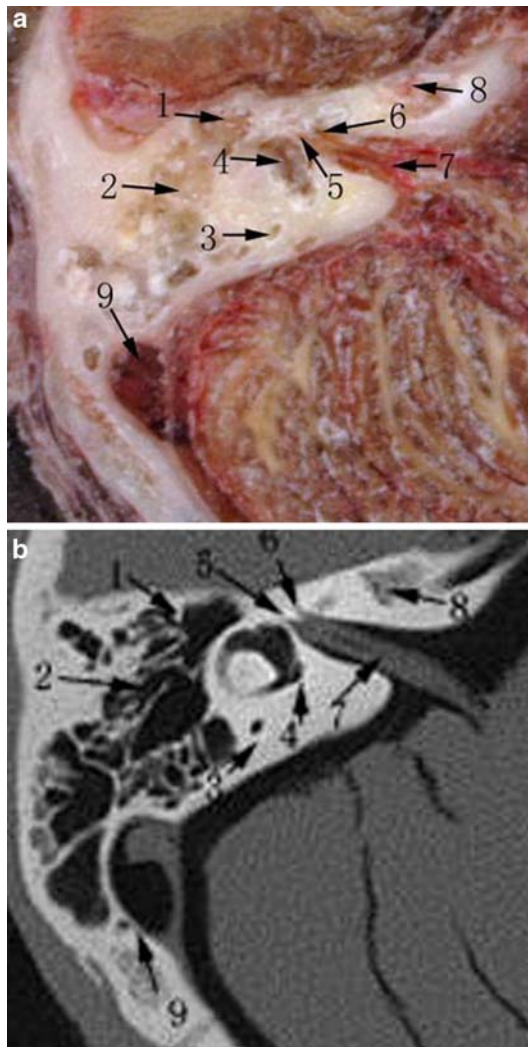


**Fig. 3** **a** Section of the superior part of fundus of internal acoustic meatus. **b** CT corresponding to **a**. 1 atticus, 2 mastoid antrum, 3 posterior semicircular canal, 4 vestibule, 5 superior vestibular nerve, 6 facial nerve internal auditory canal segment, 7 internal auditory canal, 8 trigeminal nerve, 9 sigmoid sinus

with gelatin after cry preservation. The container was filled with 5% gelatin combined with pink watercolor dye for the first layer, and 3% gelatin combined with edible blue (Methylene Blue) dye for the second, third, and fourth layer at a 24-h interval. The color of the dye was chosen as opposite and complementary to that of the specimen in order to wipe out the color of background, while, pink was contra to Methylene Blue.

Then SKC-500 numerical control milling machine (made in china, 0.001 mm for milling accuracy) was used to shave off slices of the specimen at  $-15^\circ$  in low temperature laboratory [14]. In the study, the serial axial-sections 0.1 mm in thickness were photographed with high-resolution digital camera (Canon EOS 20D, made in Japan). The data of the thin sectional anatomy was input into and saved

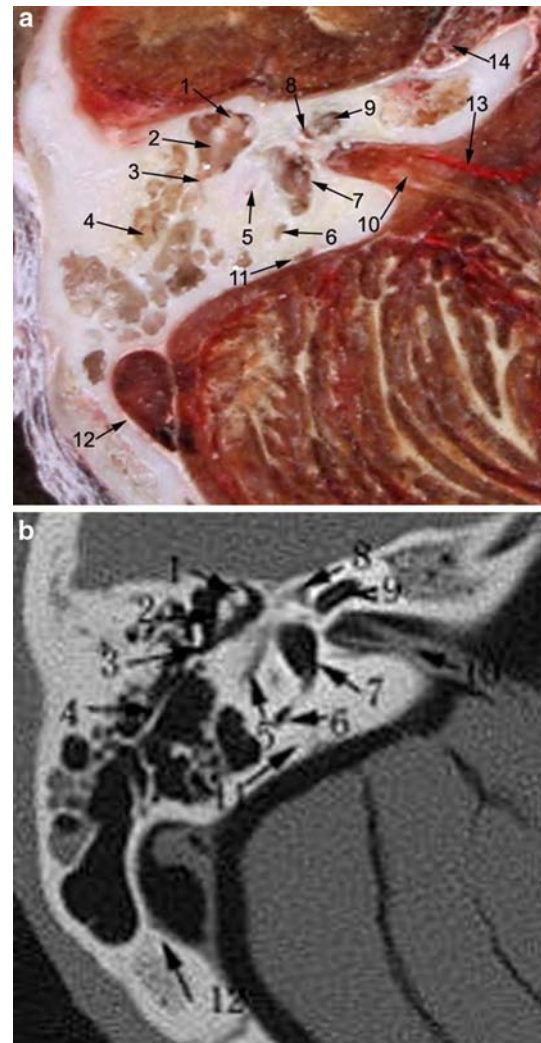


**Fig. 4** **a** Section of the malleoincudal articulation. **b** CT corresponding to **a**. 1 head of malleus, 2 short crus of incus, 3 entrance to mastoid antrum, 4 mastoid process, 5 tympanic segment of facial canal, 6 posterior semicircular canal, 7 vestibule, 8 facial nerve labyrinthine segment, 9 cochlea, 10 nervus statoacusticus, 11 vestibular aqueduct, 12 sigmoid sinus, 13 labyrinthine artery, 14 Meckel' cave

in computer (Dell) where the images were processed by Photoshop (software) and compared with the CT images.

To make sure the axial images gotten by MPR matched the thin sectional anatomy images accurately, double blind method was used. We asked an anatomy teacher and a radiologist both with 10 years of work experience to check fifty anatomical structures and compare them in thin sectional anatomy with them in CT images. They observed them, chose twenty typical sections which the thin sectional anatomy correlate with the MSCT images coincidentally, and described the intra-temporal anatomical features of these sections, and singled out the anatomical details that had been missed or overlooked or couldn't be displayed clearly.



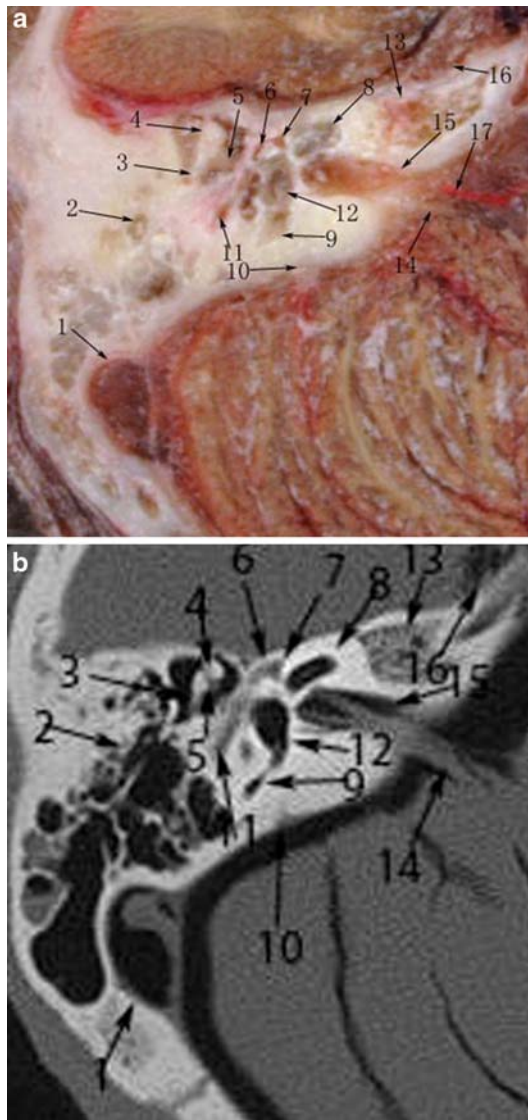


**Fig. 5** **a** Section of the geniculate ganglion. **b** CT corresponding to **a**. 1 sigmoid sinus, 2 mastoid cells, 3 short crus of incus, 4 head of malleus, 5 long crus of incus, 6 the turn-over of the facial nerve, 7 geniculate ganglion, 8 cochlea, 9 ampullar bony crura of posterior semicircular canal, 10 vestibular aqueduct, 11 facial nerve, 12 vestibule, 13 trigeminal nerve, 14 nervus statoacusticus, 15 internal auditory meatus, 16 Meckel' cave, 17 labyrinthine artery

## Results

Using the numerical control milling technique, from the emergence of petrous pyramid to the disappearance of the mastoid, we got 312, 295 and 320 slices of axial sectional anatomy, respectively, for three times of scanning, which were 0.1 mm thick. The size of the images is  $3,504 \times 2,336$  and the resolution is 8,200 thousand pixels. The color of the thin sectional images is bright, easy to observe.

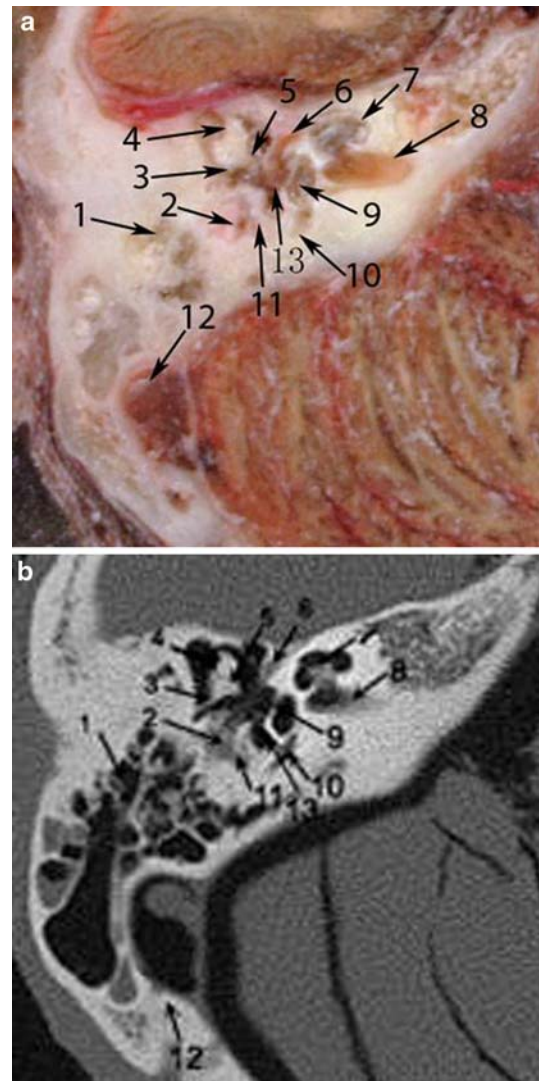


**Fig. 6** **a** Section of the vestibular window. **b** CT corresponding to **a**. 1 mastoid cells, 2 mastoid segment of facial canal, 13 short crus of incus, 4 head of malleus, 5 long crus of incus, 6 tympanic segment of facial canal, 7 cochlea, 8 internal acoustic meatus, 9 vestibular window, 10 posterior semicircular canal, 11 stapedius, 12 sigmoid sinus, 13 stapes

Seventy-eight, 73 and 80 slices of axial CT images were obtained, respectively, from the specimens. Many microstructures could be displayed clearly in these CT images, from which twenty typical sections were chosen that the thin sectional anatomy correlated with CT images coincidentally to describe in depicting the inner structures of the temporal bone. Fifty structures of the temporal bone in the thin sectional anatomy and CT images were chosen, some structures of which were difficult to be displayed, and some were easy to be missed. However, all of them can be displayed clearly and satisfactorily in both ways (Figs. 1, 2, 3, 4, 5, 6, 7, 8, 9, 10, 11, 12, Table 1).

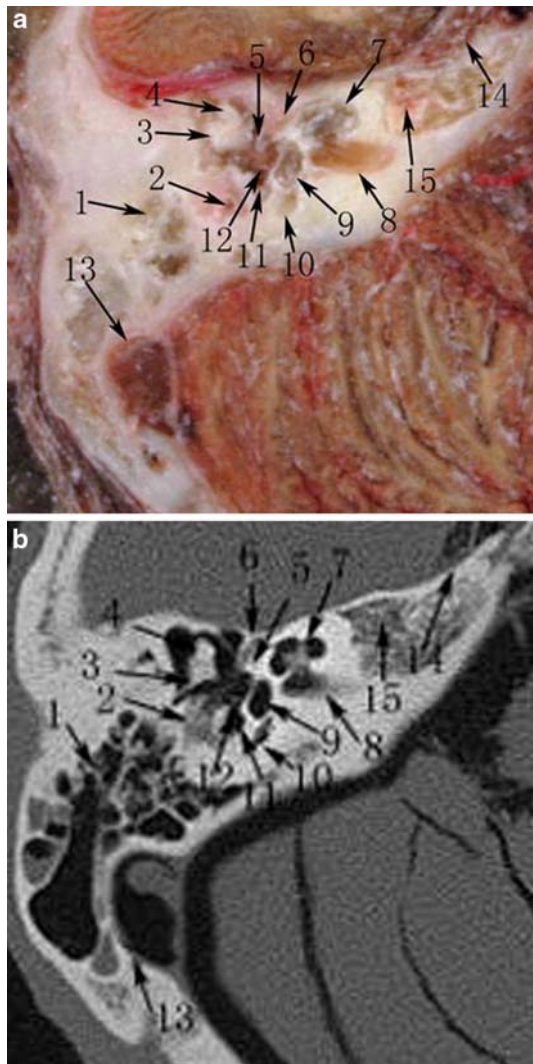


**Fig. 7** **a** Section of the cochleariform process. **b** CT corresponding to **a**. 1 mastoid cells, 2 mastoid segment of facial canal, 3 short crus of incus, 4 head of malleus, 5 cochleariform process, 6 canal for tensor tympani muscle, 7 cochlea, 8 internal acoustic meatus, 9 vestibule, 10 posterior semicircular canal, 11 sinus tympani, 12 stapes, 13 sigmoid sinus, 14 Meckel' cave

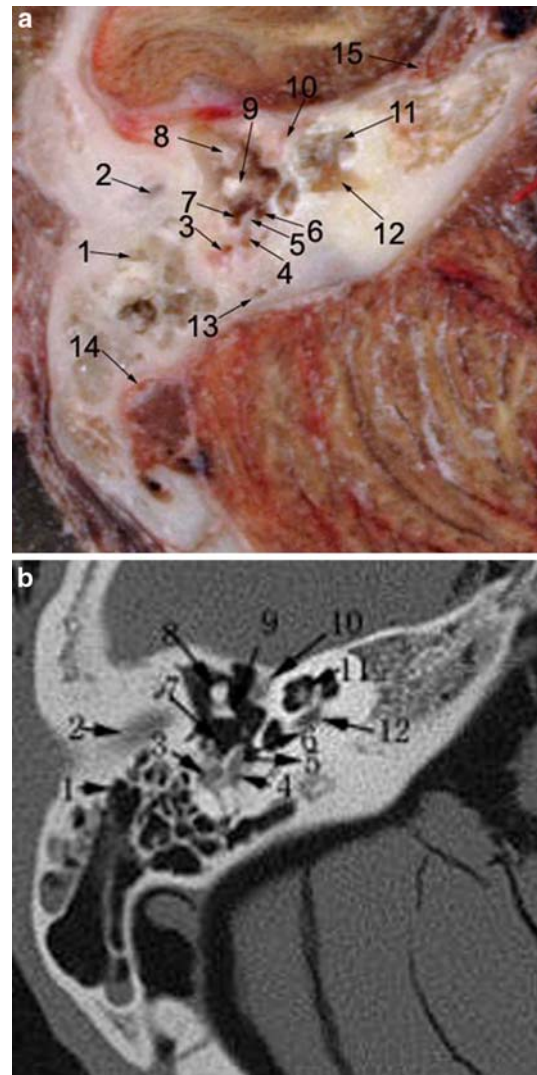


**Fig. 8** **a** Section of the pyramidal eminence. **b** CT corresponding to **a**. 1 mastoid cells, 2 external auditory canal, 3 mastoid segment of facial canal, 4 stapedius, 5 pyramidal eminence, 6 sinus tympani, 7 facial recess, 8 neck of malleus, 9 long crus of incus, 10 canal for tensor tympani muscle, 11 cochlea, 12 inner auditory meatus, 13 vestibular aqueduct, 14 sigmoid sinus, 15 Meckel' cave

## Discussion

CT is mainly depended on to diagnose the disease of the temporal bone in clinics. Now, CT can offer us three planes (axial, coronal, and sagittal plane) of the structure, even any plane. This capability lead to a reassessment of the optimal imaging planes for the depiction of temporal bone [1, 3, 6, 8, 22]. However, the axial plane is still the fundamental one [8, 11, 12, 20, 21]. Therefore we focused the study on the thin axial sectional anatomy and the correlation of between the anatomical and MSCT image, which plays an important role in recognizing the microstructures and diagnosing disease.

Recent advances in multi-slice CT allow the acquisition of isotropic voxels that can be reconstructed in any plane after volume scan. The collimator of the MSCT is 0.6 mm, increment of reconstruction is 0.1 mm, and the matrix can be enlarged to  $1,024 \times 1,024$ . With such improvements of the quality of the image, radiologists have the opportunity to visualize the anatomic structures of the temporal bone in greater detail and may help to increase the accuracy of CT for diagnosing the diseases of the middle and inner ear. It will be applied widely in the auriculotemporal medical image. In the study, we used MPR technology to adjust the CT image that did not match with the corresponding sectional anatomy [8, 11, 18]. With the improvement of the



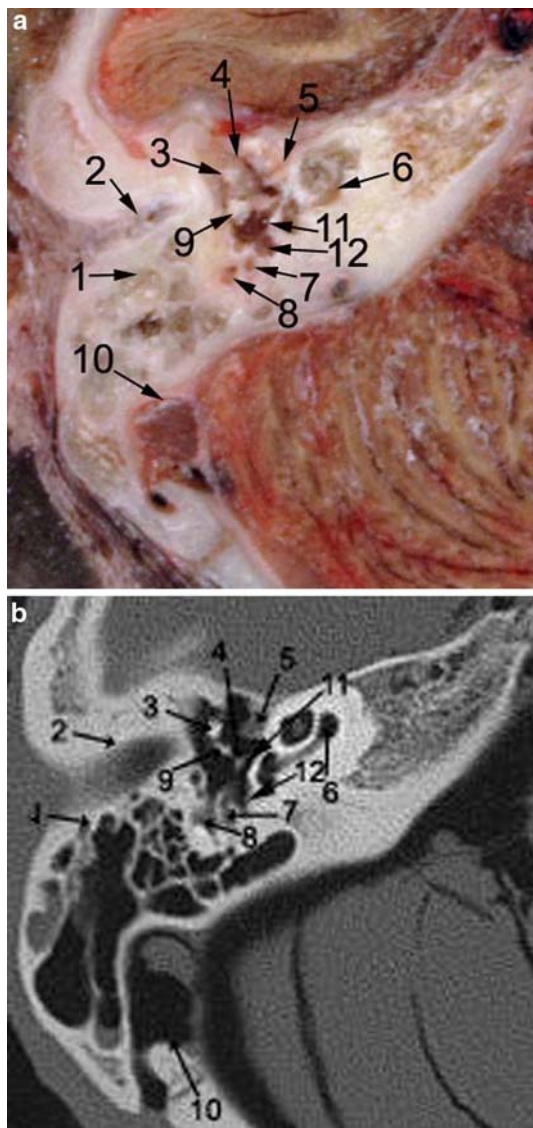


**Fig. 9** **a** Section of the tensor tympani. **b** CT corresponding to **a**. 1 mastoid cells, 2 external auditory canal, 3 malleus, 4 tympanic cavity, 5 tensor tympani, 6 cochlea, 7 stapedius, 8 mastoid segment of facial canal, 9 long crus of incus, 10 sigmoid sinus, 11 head of stapes, 12 sinus tympani

medical image, it requests the sectional anatomy to provide us with more precise and clearer information. All of these would enable us to recognize the images exactly [6, 8, 11, 12, 21], and discover some morphological changes which would be easy to be overlooked. Therefore, we had better promote the direction of the sectional anatomy with new method, which is thinner, clear and more digitalized.

There are two recent methods in the research of sectional anatomy, one is to reserve the specimens and the other is not. The frozen sectional anatomy technique can't meet the need of the medical image because of the thicker section and saw depletion, but it can preserve the specimen. The

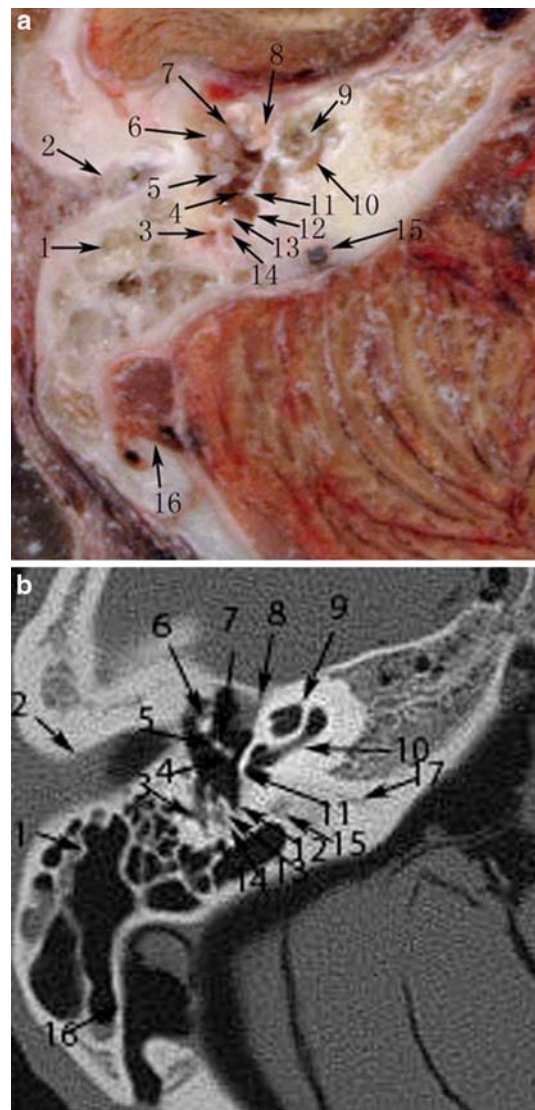


**Fig. 10** **a** Section of the basilar turn of cochlea. **b** CT corresponding to **a**. 1 mastoid cells, 2 external auditory canal, 3 mastoid segment of facial canal, 4 stapes, 5 long crus of incus, 6 malleus, 7 atticus, 8 canal for tensor tympani muscle, 9 cochlea, 10 basilar turn of cochlea, 11 promontorium tympani, 12 sinus tympani, 13 pyramidal eminence, 14 stapedius, 15 cupula of jugular fossa, 16 sigmoid sinus, 17 cochlea

thickness of the plastination slice is 1.2 mm, the saw depletion of a diamond saw thread is about 0.2 mm, and the specimen is easy to save after the processing of plastination [15]. Even though the slice is thinner, but it is cannot compete with MSCT with increment of 0.1 mm. It requires more time to make, and the specimen is easy to yield. Moreover, it is difficult for the size of the specimen to exceed 100 mm × 100 mm × 100 mm with the spatial limitation of the slicing machine. The technique of celloidin embedding demands complete decalcification to reduce the lesion of the blade and the tissue, but the long decalcifying will cause soft tissue deformation and strangulation, which

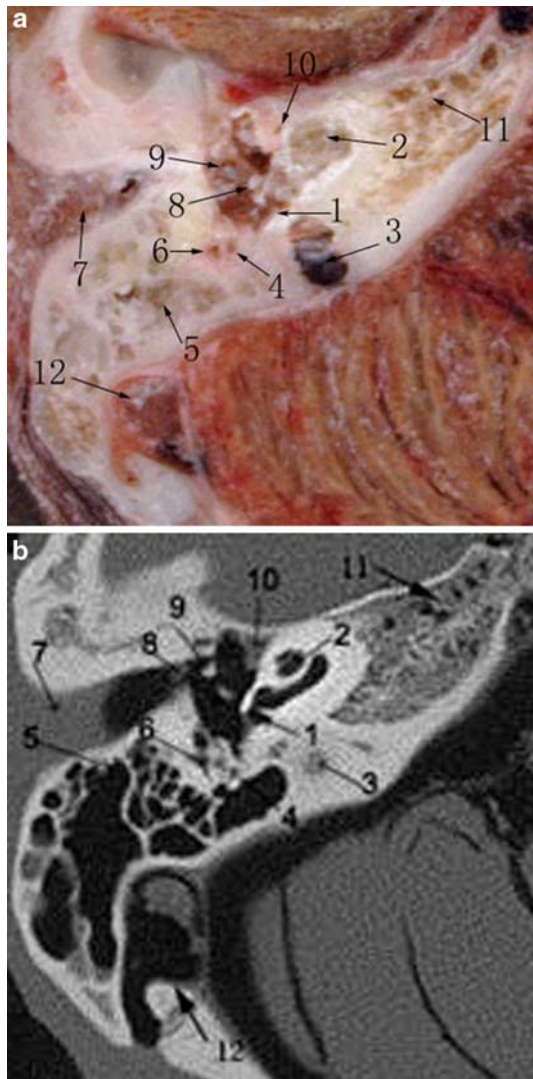


**Fig. 11** **a** Section of the round window. **b** CT corresponding to **a**. 1 round window, 2 cochlea, 3 cupula of jugular fossa, 4 stapedius, 5 mastoid cells, 6 mastoid segment of facial canal, 7 external acoustic meatus, 8 long crus of incus, 9 neck of malleus, 10 canal for tensor tympani muscle, 11 petrous bone, 12 sigmoid sinus

would influence the accuracy of the bi-dimensional image. With the plan of virtual human being put into practice, the numerical cry milling technique develops rapidly [14].

The present study has the following features: using the numerical control milling machine with precision of 0.001 mm, we could adjust the thickness of the slices from 0.001 mm to 1 mm. We chose 0.1 mm as the thickness of slices without preserving the specimen, so there was no saw depletion. Embedding without decalcification and retaining the original structures of the temporal bone is helpful to observe the anatomic structure exactly. Serial sections are beneficial for observing the spatial location and variation of the temporal bone continuously. The time consumed is short for the whole process: 5 days for freezing, 4 days for

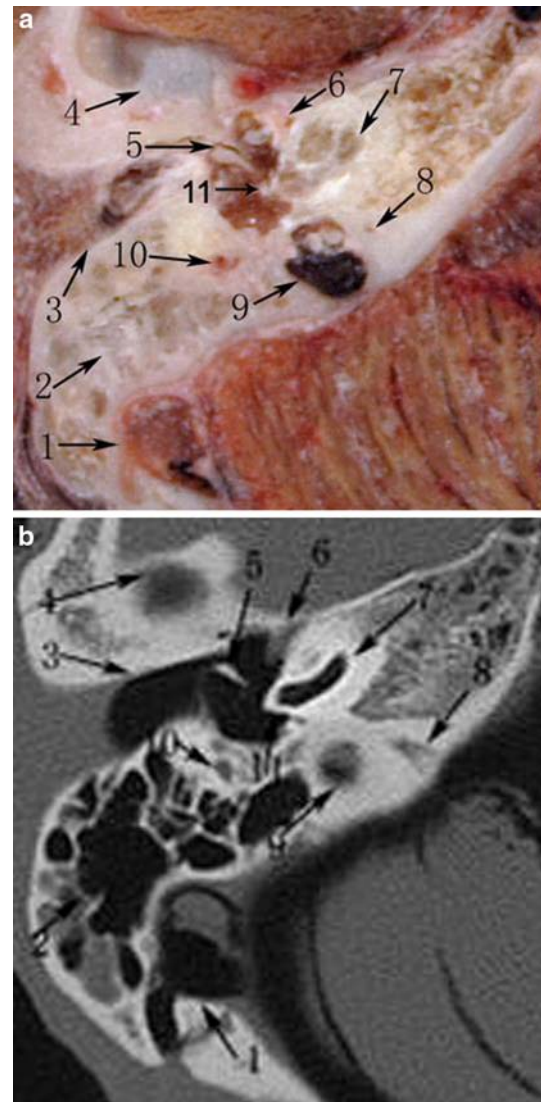


**Fig. 12** **a** Section of the manubrium of malleus. **b** CT corresponding to **a**. 1 sigmoid sinus, 2 mastoid cells, 3 external acoustic meatus, 4 temporomandibular joint, 5 manubrium of malleus, 6 canal for tensor tympani muscle, 7 cochlea, 8 aqueduct of cochlea, 9 jugular bulb, 10 mastoid segment of facial canal, 11 promontorium tympani

embedding, and 3 days for milling, and the specimens are easy to be kept fresh and unlikely to deform. The canon camera is controlled by software Canon Utilities EOS Capture, the size of the image  $3,504 \times 2,336$ , resolution about 8,200 thousand pixels, resulting in large data volume. The structures are clear, the location of the tissue is fixed, and it can display the auriculotemporal microstructures and their mutual relationships between the nerves, blood vessels and bones. The study found the sectional anatomy correlated with the images of MSCT, which helps to recognize the micro intra-temporal bone. In addition, it is helpful to reinforce the apprehension in diagnosing of auriculotemporal image. The three-dimensional images reconstructed from

**Table 1** The comparison of the grade showed by the different methods (three specimens)

Anatomic landmark	First of the specimens		Second of the specimens		Third of the specimens	
	Section	CT	Section	CT	Section	CT
Stapedius muscle	+++	+++	+++	+++	+++	+++
Stapedius tendon	+++	+++	+++	+++	+++	+++
Tensor tympani muscle	+++	+++	+++	+++	+++	+++
Tensor tympani tendon	+++	+++	+++	+++	+++	+++
Facial nerve canal: labyrinthine segment S1	+++	+++	+++	+++	+++	+++
Facial nerve canal: tympanic segment S2	+++	+++	+++	+++	+++	+++
Facial nerve canal: mastoid segment S3	+++	+++	+++	+++	+++	+++
Canal of the cochlear nerve	+++	+++	+++	+++	+++	+++
Canal of the superior division of the vestibular nerve	+++	+++	+++	+++	+++	+++
Canal of the saccular nerve	+++	+++	+++	+++	+++	+++
Canal of the posterior ampullary nerve	+++	+++	+++	+++	+++	+++
Canal of the accessory nerve of the posterior ampullary nerve	+++	+++	+++	+++	+++	+++
Malleus head	+++	+++	+++	+++	+++	+++
Malleus neck	+++	+++	+++	+++	+++	+++
Manubrium of malleus	+++	+++	+++	+++	+++	+++
Lateral process of malleus	+++	+++	+++	+++	+++	+++
Anterior process of malleus	+++	+++	+++	+++	+++	+++
Incus body	+++	+++	+++	+++	+++	+++
Short process of incus	+++	+++	+++	+++	+++	+++
Long process of incus	+++	+++	+++	+++	+++	+++
Lenticular process of incus	+++	+++	+++	+++	+++	+++
Incudomalleolar articulation	+++	+++	+++	+++	+++	+++
Stapes head	+++	+++	+++	+++	+++	+++
Anterior crus of stapes	+++	+++	+++	+++	+++	+++
Posterior crus of stapes	+++	+++	+++	+++	+++	+++
Stapes footplate	+++	+++	+++	+++	+++	+++
Incudostapedial articulation	+++	+++	+++	+++	+++	+++
Tympanic membrane	+++	+++	+++	+++	+++	+++
Oval window	+++	+++	+++	+++	+++	+++
Round window	+++	+++	+++	+++	+++	+++
Round window niche	+++	+++	+++	+++	+++	+++
Tegmen tympani	+++	+++	+++	+++	+++	+++
Pyramidal eminence	+++	+++	+++	+++	+++	+++
Cochleariform process	+++	+++	+++	+++	+++	+++
Osseus spiral lamina of cochlea	+++	+++	+++	+++	+++	+++
Modiolus of cochlea	+++	+++	+++	+++	+++	+++
Mastoid cells	+++	+++	+++	+++	+++	+++
Cochlear aqueduct	+++	+++	+++	+++	+++	+++
Vestibular aqueduct	+++	+++	+++	+++	+++	+++
Groove of the greater superficial petrousal nerve	+++	+++	+++	+++	+++	+++
Anterior bony ampulla	+++	+++	+++	+++	+++	+++
Posterior bony ampulla	+++	+++	+++	+++	+++	+++
Lateral bony ampulla	+++	+++	+++	+++	+++	+++
Petromastoid canal	+++	+++	+++	+++	+++	+++



**Table 1** continued

Anatomic landmark	First of the specimens		Second of the specimens		Third of the specimens	
	Section	CT	Section	CT	Section	CT
Labyrinthine artery	+++	+++	+++	+++	+++	+++
Common bony crus	+++	+++	+++	+++	+++	+++
Geniculate ganglion	+++	+++	+++	+++	+++	+++
Facial recess	+++	+++	+++	+++	+++	+++
Promontorium tympani1	+++	+++	+++	+++	+++	+++
Meckel' cave	+++	+++	+++	+++	+++	+++

The whole structure or almost whole structure was shown, above 76% of the whole structure, grade as +++; most part of the structure was shown, 51–75%, graded as ++; little part of the structure was shown, 26–50%, graded as +; almost shows nothing, below 25%, graded as –

these data can supply the surgeon with accurate morphologic pre-operative information, as well as provide the landmark of the surgical approach in the skull base operation [1, 3, 22, 24, 25]. It can be applied to stereology, and the slices acquired can be sent to the image analysis system of the computer, so that it can be easily applied to the analysis and measurement. It can delineate the relationship between the internal structures and the temporal bone [6, 13, 16–18].

We got 312, 295 and 320 slices from three heads, respectively, using the numerical control milling technique in our study, and 78, 73 and 80 slices of CT image. We chose one section from those similar sections to match the CT image, whereas the serial sections are helpful to observe the spatial variation of the intra-temporal bone [9, 13, 14, 16, 18]. The complicated spatial distribution of these structures could be sequentially manifested in different thin laminae of the successive axial images, which helps to their clear depiction through MPR adjustment following CT isotropic scan. One time scan in any direction and reconstruction could both fully satisfy the requirement of doctors and decrease the radiation received by patients at the same time.

As a result of the rapid development of sectional anatomy and imageology, certain intricate structures that are overlooked or in no way of being displayed during the past studies could be depicted in the successive images of sub-millimeter thin laminar sectional anatomy and MSCT [7, 17]. To explain this, two reasons can be introduced: firstly, in the past, the lamina of sectional anatomy and CT images were too thick; secondly, the clinical medicine progress urgently required displaying certain structures. In our study, we demonstrated that many delicate structures of human body, which are closely related to clinical practice, could be displayed in either way mentioned above. For example, the round window, footplate complex of stapes, stapedius muscle, facial recess, cochleariform process, geniculate ganglion, modiolus of cochlea, superior vestibular nerve, petromastoid canal, cochlear aqueduct, sulcus for superior petrosal sinus, tensor tympani muscle, vestibular

aqueduct, incudomalleolar articulation, common bony crus and cochlear aqueduct could all be shown in the following images. All these structures are helpful for the diagnosis of some diseases and determination of surgical schemes [2, 4, 19, 23]. Besides, some of them are very important anatomic landmarks that are not only potential operative approaches or passageways but also could contribute to avoiding surgical injuries of some major structures. One good illustration is the neighboring relationship among the horizontal segment of facial nerve, cochleariform process and facial recess, another is the close relationship of facial recess, round window, cochleariform process, geniculate ganglion, modiolus of cochlea and cochlear aqueduct with artificial electrical cochlea implantation. The operative route for artificial cochlear implantation has two approaches, the facial recess and the external auditory canal. The former one is attracting more and more attention owing to carrying out of artificial cochlear implantation. The facial recess, characterized as extremely narrow, is of vital importance due to its adjacent anatomic structures, the facial nerve and the chorda tympani nerve, which makes the depth of facial recess a determinative factor for an easy operative approach. What's more, estimation of its depth could provide more options for surgery before operation. Through facial recess, the round window with its front promontorium tympani and the basal turn of the cochlear can all be seen distinctly, which makes it possible to drill holes on the tympanic scala of the basal turn of the cochlear. The facial recess approach is ideal for artificial cochlear implantation in that its adjoining round window niche facilitates the electrode insertion under direct viewing. However, the facial nerve should be taken care of during the operation, since the approach is approximate to the facial nerve canal. In recent years, the newly developed electric cochlear implantation claims higher requirement for more accurate measurement and location of round window. Identification of the location as well as anatomic correlations between round window area and its related structures on transverse thin

lamina and CT images of ears could offer anatomic reference for both imaging diagnosis and surgical treatments.

## Conclusion

Despite the limitations of the study, such as lack of a large sample that may diminish the statistical efficiency, we still can draw a conclusion that the thinner, clear and sub-millimeter images of sectional anatomy and MSCT can be obtained by this methodology.

## References

- Alexander AE Jr, Caldemeyer KS, Rigby P (1998) Clinical and surgical application of reformatted high-resolution CT of the temporal bone. *Neuroimaging Clin North Am* 8(3):631–650
- Briggs RJ, Tykocinski M, Stidham K et al (2005) Cochleostomy site: implications for electrode placement and hearing preservation. *Acta Otolaryngol* 125(8):870–876
- Chan LL, Manolidis S, Taber KH et al (2001) Surgical anatomy of the temporal bone: an atlas. *Neuroradiology* 43(10):797–808. DOI 10.1007/s002340100631
- Colletti V, Soli SD, Carner M et al (2006) Treatment of mixed hearing losses via implantation of a vibratory transducer on the round window. *Int J Audiol* 45(10):600–608
- Fatterpekar GM, Mukherji SK, Lin Y et al (1999) Normal canals at the fundus of the internal auditory canal: CT evaluation. *J Comput Assist Tomogr* 23(5):776–780
- Gunlock MG, Gentry LR (1998) Anatomy of the temporal bone. *Neuroimaging Clin North Am* 8(1):195–209
- Sick H, Veillon F (1989) Atlas of slices of the temporal bone and adjacent region. Anatomy and computed tomography. Bergmann-Springer Verlag, pp 5–45
- Jager L, Bonell H, Liebi M et al (2005) CT of the normal temporal bone: comparison of multi- and single-detector row CT. *Radiology* 235(1):133–141
- Jun BC, Song SW, Cho JE et al (2005) Three-dimensional reconstruction based on images from spiral high-resolution computed tomography of the temporal bone: anatomy and clinical application. *J Laryngol Otol* 119(6):693–698
- Koesling S, Kunkel P, Schul T (2005) Vascular anomalies, sutures and small canals of the temporal bone on axial CT. *Eur J Radiol* 54(3):335–343
- Lane JJ, Lindell EP, Witte RJ et al (2006) Middle and inner ear: improved depiction with multiplanar reconstruction of volumetric CT data. *Radiographics* 26(1):115–124
- Powitzky ES, Hayman LA, Bartling SH et al (2006) High-resolution computed tomography of temporal bone: Part III: axial postoperative anatomy. *J Comput Assist Tomogr* 30(2):337–343
- Parlier-Cuau C, Champsaur P, Perrin E et al (1998) High-resolution computed tomography of the canals of the temporal bone: anatomic correlations. *Surg Radiol Anat* 20(6):437–444. DOI 10.1007/BF01653137
- Qiu MG, Zhang SX, Liu ZJ, et al (2004) Visualization of the temporal bone of the Chinese Visible Human. *Surg Radiol Anat* 26(2):149–152. DOI 10.1007/s00276-003-0188-9
- Qiu MG, Zhang SX, Liu ZJ et al (2003) Plastination and computerized 3D reconstruction of the temporal bone. *Clin Anat* 16(4):300–303. DOI 10.1002/ca.10076
- Reisser C, Schubert O, Forsting M et al (1996) Anatomy of the temporal bone: detailed three-dimensional display based on image data from high-resolution helical CT: a preliminary report. *Am J Otol* 17(3):473–479
- Robert Ruben, Jan J Grote, Johannes Land (1995) Interactive anatomy. Atlas of continuous cross-sections. Ed Elsevier, pp 35–70
- Rodt T, Ratiu P, Becker H et al (2002) 3D visualisation of the middle ear and adjacent structures using reconstructed multi-slice CT datasets, correlating 3D images and virtual endoscopy to the 2D cross-sectional images. *Neuroradiology* 44:783–790. DOI 10.1007/s00234-002-0784-0
- Roland PS, Wright CG (2006) Surgical aspects of cochlear implantation: mechanisms of insertional trauma. *Adv Otorhinolaryngol* 64:11–30
- Seemann MD, Seemann O, Bonél H, et al (1999) Evaluation of the middle and inner ear structures: comparison of hybrid rendering, virtual endoscopy and axial 2D source images. *Eur Radiol* (9):1851–1858. DOI 10.1007/s003300050934
- Swartz JD, Harnsberger HR, Mukherji SK (1998) The temporal bone: contemporary diagnostic dilemmas. *Radiol Clin North Am* 36(5):819–853
- Schubert O, Sartor K, Forsting M et al (1996) Three-dimensional computed display of otosurgical operation sites by spiral CT. *Neuroradiology* 38(7):663–668. DOI: 10.1007/s002340050330
- Toth M, Alpar A, Patonay L et al (2006) Development and surgical anatomy of the round window niche. *Ann Anat* 188(2):93–101
- Vrionis FD, Foley KT, Robertson JH et al (1997) Use of cranial surface anatomic fiducials for interactive image-guided navigation in the temporal bone: a cadaveric study. *Neurosurgery* 40(4):755–764
- Woolley AL, Oser AB, Lusk RP et al (1997) Preoperative temporal bone computed tomography scan and its use in evaluating the pediatric cochlear implant candidate. *Laryngoscope* 107(8):1100–1106